

Tumor therapy by fast moving magnetic nanoparticle under low-frequency alternating magnetic field

Yangyang Liu, Zhiyu Qian*, Jianhua Yin and Xiao Wang
Department of Biomedical Engineering
Nanjing University of Aeronautics and Astronautics
Nanjing, P. R. China
**zhiyu@nuaa.edu.cn*

Received 13 March 2014
Accepted 17 June 2014
Published 15 July 2014

Magnetic nanoparticle plays an important role in biomedical engineering, especially in tumor therapy. In this paper, a new technique has been developed by using the rapid moving magnetic nanoparticle under a low-frequency alternating magnetic field (LFAMF) to kill tumor cells. The LFAMF system which was used to drive magnetic nanoparticles (MNPs) was setup with the magnetic field frequency and power range at $\sim 10\text{--}100$ Hz and $\sim 10\text{--}200$ mT, respectively. During the experiment, the LFAMF was adjusted at different frequencies and power levels. The experimental results show that the liver tumor cells (HepG2) mixed with MNPs ($10\ \mu\text{g}/\text{mL}$) became partial fragments when exposed in the LFAMF with different frequencies ($\sim 10\text{--}100$ Hz) and power ($\sim 10\text{--}200$ mT), and the higher the frequency or the power, the more the tumor cells were killed at the same magnetic nanoparticle concentration. Conclusion: Tumor cells were effectively damaged by MNPs under LFAMF, which suggests that they had great potential to be applied in tumor therapy.

Keywords: Different frequency; cells; power; cancer.

1. Introduction

Radiotherapy and chemotherapy are mostly used for cancer treatment. However, both methods are not optimal as they damage normal tissue and produce a series of adverse reactions while damaging tumor cells. As a result, much effort has been devoted to the research of more efficient cancer therapies. Nanotechnology approaches are currently the most promising.^{1–5} The use of nanoparticles has attracted more attention due to their inherent

ultra-fine size, optical characteristics, biocompatibility, and magnetic properties.^{6,7} Amongst nanoparticles, magnetic nanoparticles (MNPs) is the choice of many researchers. MNPs share special properties such as strong magnetic responsiveness, high saturation field, and no magnetic interaction after the external magnetic field is removed.^{8,9} The functional properties of the MNPs can be applied for specific biological functions, such as drug delivery, hyperthermia, magnetic targeting, magnetic

This is an Open Access article published by World Scientific Publishing Company. It is distributed under the terms of the Creative Commons Attribution 3.0 (CC-BY) License. Further distribution of this work is permitted, provided the original work is properly cited.

resonance imaging (MRI), cell labeling and sorting, and immunoassays.^{10–12} The cytotoxicity and efficiency of MNPs are important criteria to take into account for their biomedical application, which depends upon the nanoparticles' structure, functionality, stability, and dispensability. Results about toxicity and biological safety of MNPs show that they are relatively safe.^{13,14}

Nowadays there is a growing concern on heat treatment, which is one of the most promising approaches to practical cancer therapy.^{15–17} There is no doubt that MNPs are used as effective heat generators because of their high degree of incorporation into cancer cells and heating efficiency under an external high frequency alternating magnetic field.¹⁸ Therefore, the application of MNPs for hyperthermia treatment was investigated in the work of Chan *et al.* and Jordan *et al.* in 1993.^{19,20} These studies experimentally proved the high efficiency of a magnetic crystal suspension to absorb the energy of an alternating magnetic field and converted it into heat. However, hyperthermia is not currently applied in clinical medical field because it is difficult to control the temperature of nanoparticles during tumor treatment and is not easy to get effective damaging temperatures *in vivo*. Until now many researchers have tried to find out new ways to cope with these difficulties.

On the other hand, the functional/structural changes of essential cellular components (the plasma membrane and other cellular organelles) which can be considered a “vulnerable site” may threaten the functioning of the cellular unit and even induce cell death. Many studies have shown that there are ways to produce irreversible effects on cell membranes. Electric impulses (8 kV/cm, 5 μ s) were found to increase greatly the uptake of DNA into cells, but this was a reversible process.²¹ If a periodic electric field is applied on the cell instead, increasing voltage will change the electrical charge on cell membrane. When the pulse time is shortened, micro pore will be difficult to heal and cell membrane structure will develop irreversible damage.

We propose a special method, based on MNPs and magnetic fields, to produce irreversible damage to tumor cell membranes. MNPs will produce rapid movements or local vibrations along with an external magnetic field.²² A low-frequency alternating magnetic field (LFAMF), used for its low heating efficiency, has previously been designed.^{23–25} The speed and direction of moving MNPs are changed

by adjusting the magnetic field power and magnetic field frequency, resulting in tumor cells injury and cell membrane damage.^{26–29} The method has bright spots as follows: (1) The frequencies and power of alternating magnetic field take together and pass harmlessly through the tissues containing MNPs; (2) This physical way destroys the tumors with no chemical effect and radiation effect. This additional feature opens up possibilities for the development of multi-functional and multi-therapeutic approaches for treating a number of diseases.

In this study, the sample of liver tumor cell HepG2 was introduced. HepG2 cell's injury by magnetic Fe₃O₄ nanoparticles (MNP-Fe₃O₄) under LFAMF with different magnetic field intensities and frequencies has been investigated.

2. Materials and Methods

2.1. Setup

A LFAMF generator was developed for obtaining alternating magnetic field gradient. In most cases, the magnetic field gradient is generated by a ferrite core in excitation winding. The particles, usually in the form of a biocompatible ferrofluid are incubated with cells. When the ferrite core approaches the culture plate, the MNPs begin rapid movements, which are caused by external alternating magnetic fields.

The setup base mentioned above is designed as follows. MCU drives an H bridge circuit to produce an alternating current flowing in the coil. Ferrite core in excitation winding enhances the LFAMF intensity at the gap between the magnetic poles. According to wire specifications table, the following formula in our calculations (Eq. (1)) was adopted,

$$B = \text{Greek}(m)H = \text{Greek}(m)NI/L, \quad (1)$$

where B is the magnetic induction intensity, $\text{Greek}(m)$ is the relative magnetic permeability, H is the magnetic field intensity, N is the number of turns of the coil, l is the effective magnetic circuit and L is the current flowing in the coil. From the above equation, we designed the winding that is composed of 1250 rounds with 1 mm diameter and a matching magnetic core with 120 mm length, 80 mm width and 30 mm thickness. The current flowing in the coil is 0.5–1.2A. When the current is 1.2A, the magnetic field power is 359.2 mT in theory. During the experiment the maximal value is set to be 1A, and

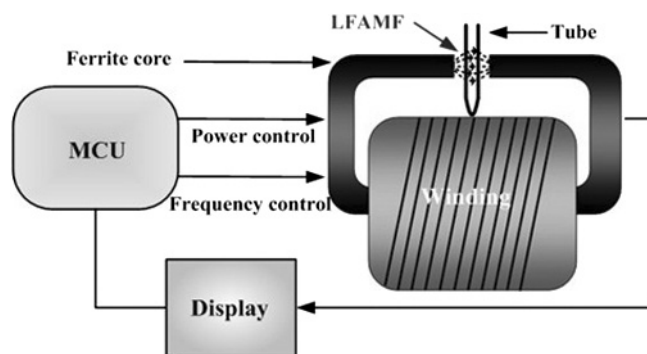


Fig. 1. Schematic diagram of LFAMF generator.

magnetic field power is 200 mT measured by gauss meter, accordingly. The placement is shown in Fig. 1, and test tube is put into the gap between two magnetic poles. The gap has a size of 20 mm length, 15 mm width and 30 mm thickness.

2.2. Preparation of MNP-Fe₃O₄

MNP-Fe₃O₄ was purchased from Nanjing Emperor Nano Material Limited Company. The particle diameter was controlled in the range of 10–50 nm. The morphology of MNP-Fe₃O₄ was characterized using transmission electron microscopy (TEM). Before TEM measurement, the nanoparticles were dispersed into distilled water, and then they were dropped on a copper-grid-supported perforated transparent carbon foil. Based on TEM images the average size of particles was confirmed.

2.2.1. Cell culture

HepG2 hepatic cancer cells were generously provided by China Pharmaceutical University. These cells were maintained as monolayer culture in RPMI 1640 medium supplemented with 10% fetal bovine serum and 1% penicillin–streptomycin at 37°C in a humidified atmosphere (5% CO₂).

2.2.2. Cellular uptake of MNP-Fe₃O₄

HepG2 cells (5×10^5 /mL) were washed twice with RPMI 1640 and seeded in a culture dish at 37°C (5% CO₂) until adhesion. Then MNP-Fe₃O₄ (10 µg/mL) was added to the dish. After 8 h of incubation with particles, the cells were washed with PBS twice, and observed by an Olympus IX51 microscope.

HepG2 cells were fixed with 2.5% glutaraldehyde in 0.1 mol sodium cacodylate buffer supplement

with 1.4% sucrose, then incorporated in agar and further processed for standard Epon embedding. Ultrathin sections (60 nm) were double stained with 1% uranyl acetate and lead citrate. Ultra-structure examination by TEM was performed with a Morgagni 268 transmission electron microscope (FEI Co) at 60 kV.

2.2.3. Viability assay

Viability assay was carried out in a 96-well plate. After adhesion, cells were incubated with different concentrations of the particles for 24 h, then with MTT (3-(4,5-Dimethylthiazol-2-yl)-2,5-diphenyltetrazolium bromide) (0.5 mg/mL) for another 3 h. Subsequently, after the medium was discarded, the same volume of DMSO was added to dissolve the formed formazan crystals. The optical density of the supernatant was read at 540 nm using a microplate spectrophotometer. Results were expressed as the percentage of the viability of treated cells relative to untreated cells.

2.3. LFAMF exposure

HepG2 cells were seeded in a big culture plate at 37°C (5% CO₂) until adherence. MNP-Fe₃O₄ (10 µg/mL) was added to the plates. After 8 h of incubation with particles, the cells were washed twice with PBS and dispensed into some small plates after digestion. The cells underwent magnetic field irradiation at different frequencies and different strengths during the same time. The related parameters are listed in Table 1.

Three kinds of field power were chosen at two kinds of frequencies, which were 10, 100 and 200 mT at 10 Hz and 10, 100 and 200 mT at 100 Hz, respectively. The experimental time was 120 min. Control groups 1 and 2 that exclude MNPs were irradiated by LFAMF. Cells in control group 3 were

Table 1. Experiment groups.

	Control group 1	Control group 2	Control group 3	10 Hz	100 Hz
Concentration/ (µg/mL)	0	0	10	10	10
LFAMF/(mT)	10	100	0	10	10
				100	100
				200	200

incubated with MNPs, but without LFAMF treatment. All of them were observed by the microscopy.

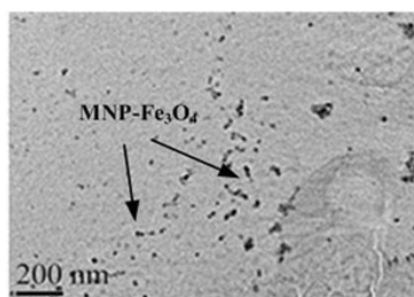
3. Results

3.1. Characteristic of $MNP-Fe_3O_4$

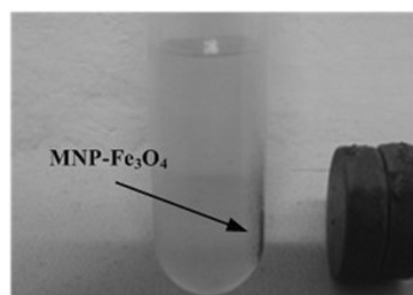
MNPs have considerable potential in their various biomedical applications due to their narrow size and shape distribution, high magnetization, and inherent biocompatibility.^{30,31} Figure 2(a) shows the purified and unmodified $MNP-Fe_3O_4$ that is observed with TEM. Average diameter of the particles is 20 nm and particles are relatively homogeneous. As single domain particles, this magnetite $MNP-Fe_3O_4$ has a strong and relatively stable magnetic moment.³² Obviously, the particles are mutually attracted and aligned with the opposite magnetic poles facing each other, as shown in Fig. 2(b).

3.2. Uptake and cytotoxicity of $MNP-Fe_3O_4$

Uptake of $MNP-Fe_3O_4$ by HepG2 cells was directly confirmed using the transmission electron microscopy (when it first appeared in the TEM) and the



(a)



(b)

Fig. 2. TEM image of $MNP-Fe_3O_4$ (a) and Magnetic attraction of $MNP-Fe_3O_4$ (b).

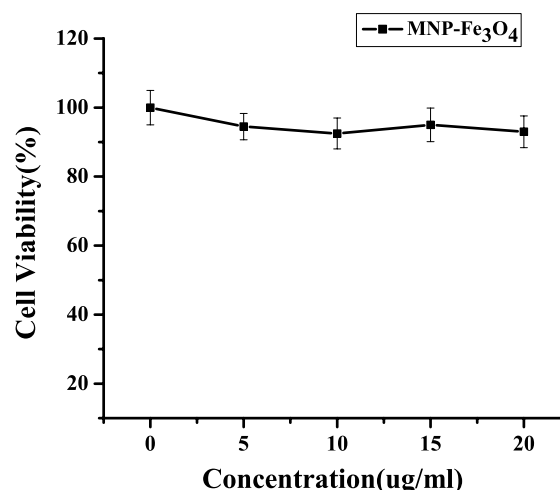


Fig. 3. Observation of $MNP-Fe_3O_4$ internalized HepG2 cells using MTT.

optical microscopy. $MNP-Fe_3O_4$ was successfully internalized into HepG2 cells. The cytotoxicity of the $MNP-Fe_3O_4$ was measured from control cells without particle treatment, which was normalized to 100% viability. As shown in Fig. 3, the $MNP-Fe_3O_4$ does not affect the viability of HepG2 cells up to the concentration of 20 $\mu\text{g}/\text{mL}$ in 24 h. They belonged to nontoxic biological materials.

Most internalized $MNP-Fe_3O_4$ was localized around cells in all sectional view of the optical microscopy. In addition, it was observed by TEM that $MNP-Fe_3O_4$ was localized in the cells as shown in Fig. 4. To further confirm the intracellular localization of $MNP-Fe_3O_4$ in HepG2 cells, another TEM study was performed. After 24 h exposure of HepG2 cells with 10 $\mu\text{g}/\text{mL}$ $MNP-Fe_3O_4$, the cells were examined by TEM. Clusters of $MNP-Fe_3O_4$ were still localized in the cells and no other changes of cellular morphology were observed in both type of investigated $MNP-Fe_3O_4$. TEM images confirmed that

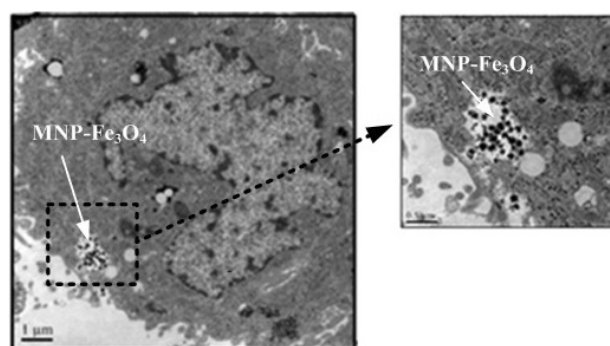


Fig. 4. TEM image of $MNP-Fe_3O_4$ internalized HepG2 cells.

large quantities of MNPs- Fe_3O_4 crossed cell membranes, consistent with the reported literature.³³

3.3. Tumor cells injury induced by MNP- Fe_3O_4 and LFAMF

Control groups 1 and 2 are shown in Figs. 5(a) and 5(b). It is found that little cells become round, and other adherent cells grow well because the cells are spindle-shaped and the structure of membranes is complete. Control group 3 is shown in Fig. 5(c) in which the cells continue to adhere with uniform size, shape and maintain the complete cell membranes.

It was noticed that, with increasing magnetic field power and frequency, there was a corresponding change in the morphology of cells. Comparing the cells under irradiation of 10 mT at 10 Hz [Fig. 5(d)]

with the control groups [Figs. 5(a)–5(c)], most cells were still alive. After irradiation of 100 mT at 10 Hz [Fig. 5(e)] and 200 mT at 10 Hz [Fig. 5(f)], a little more cells became floating, but most cells did not turn round. Comparing the cells under irradiation of 10 mT at 100 Hz [Fig. 5(g)] with the control groups, some cells turned round and floated obviously. Meanwhile, the number of cells declined. After irradiation of 100 mT at 100 Hz [Fig. 5(h)] and 200 mT at 100 Hz [Fig. 5(i)], the cell's density displayed a significant decrease over 120 min. Also due to the increase in field power and frequency, an irradiation of 200 mT at 100 Hz field was able to enhance the particle's ability to damage the cell membranes compared to that of 10 mT at 10 Hz field. As shown in Fig. 5(i) HepG2 cells became partial fragments induced under LFAMF irradiation

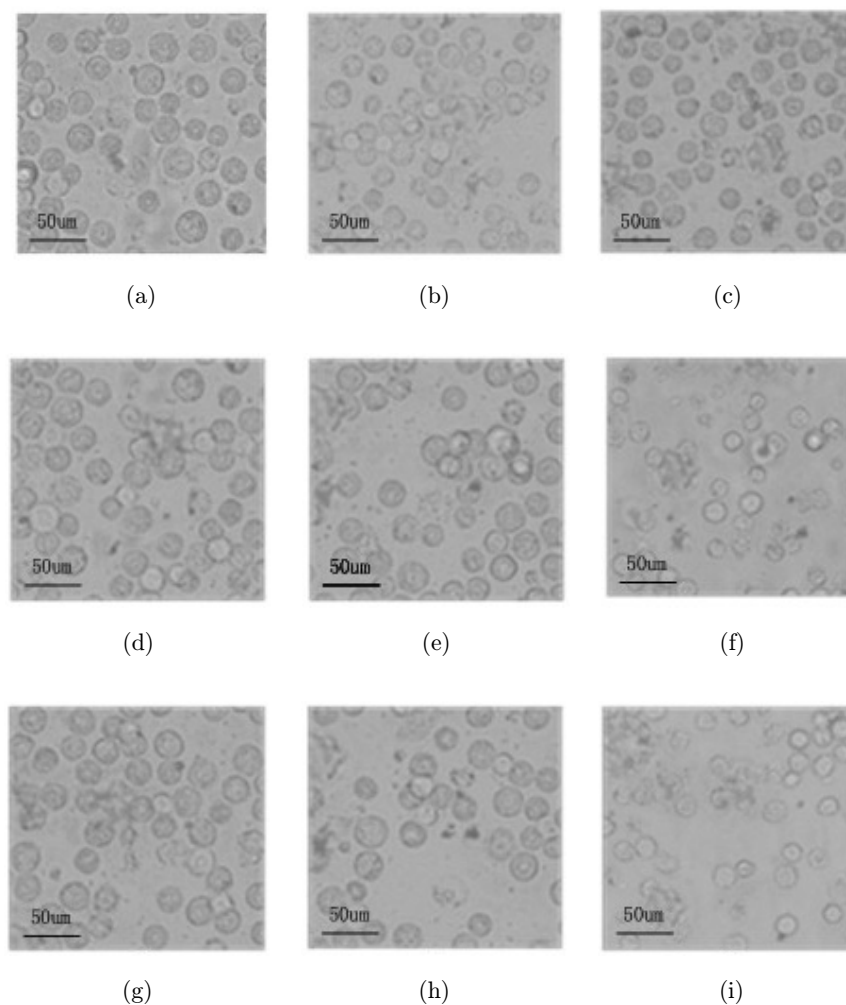


Fig. 5. Photomicrographs of cells after treatment under different LFAMF irradiation ($\times 400$): (a) control group 1, (b) control group 2, (c) control group 3, (d) at 10 mT and 10 Hz (e) at 100 mT and 10 Hz (f) at 200 mT and 10 Hz, (g) at 10 mT and 100 Hz (h) at 100 mT and 100 Hz (i) at 200 mT and 100 Hz.

of 200 mT and 100 Hz, but the structure was kept intact at 10 mT and 100 Hz [Fig. 5(g)].

4. Discussion

As far as my knowledge is concerned, MNP-Fe₃O₄ is especially susceptible to induce localized physical injury based on LFAMF, which may potentially destroy the tumors with fewer side effects and prior to radiation or chemo-therapies. MTT was used to test the toxicity of MNPs, which was proposed in 1983 by Mosmann³⁴ and has been widely used in activity detection, drug screening, tumor cell toxicity test, and radiation sensitivity measurement. By this method, the cell viability was achieved, so as to predict the compatibility of MNP-Fe₃O₄ in biological application. The results showed that different concentrations (2.5, 5, 10, 20 μg/mL) of MNP-Fe₃O₄ had no obvious effect on cell proliferation.

MNP-Fe₃O₄ and HepG2 cells were observed after 8 h, and some particles were found in large bubble structure, while they were not found in the nucleus. After 24 h, the phenomenon did not change. Hence, we would better come to the conclusion that MNP-Fe₃O₄ did not affect important functions (such as chromosome function), but the mechanism of particles entering into the cell is not yet very clear.^{35,36}

During this experiment, cultured cells were divided into nine parts, including three control groups and six experiment groups. In control groups 1 and 2, the cells were only under LFAMF irradiation during 120 min. Cells were the same under the optical microscope before irradiation, and especially the cellular structure was complete. Hence, tumor cells injury was induced by MNPs and LFAMF. Under the identical magnetic field intensity, cell injury effect was enhanced when the frequency of magnetic field increases. During the same time of the LFAMF irradiation, effects of different power on cell survival were different. Small power caused little effect on the cells. With increasing power, cell proliferation was restrained obviously. We suspect the reason is that the fast movement of MNPs under LFAMF would damage the cells physically such as changing the structure of the plasma membrane or entering the nucleus, which could be a cause of cell death.³⁷ Although the new tumor therapy was proved to be valid, more experiments are needed to explore the mechanisms on tumor cells damage.

Moreover, the mechanism of LFAMF is needed to be discussed. Because of the diamagnetic properties of cell membrane structure, an external static magnetic field (SMF) with moderate strength (1 mT–1T) is supposed to influence the viability of cells.³⁸ In this study, the complete structure of tumor cells had been destroyed with MNP-Fe₃O₄ under the exposure of LFAMF. However, extremely low-frequency magnetic fields also have a transient effect on cells.^{39–42} Differently, this paper applied a higher magnetic field strength on tumor cells, and this might cause irreversible tumor cells injuries. In addition, prolonged stimulation led to more dramatic decrease in viability, since it had been proved that the extremely low frequency magnetic fields formed irreversible membrane pores. It needs more work to study how the LFAMF works.

Considering hyperthermia treatment, MNPs generate heat in an alternating magnetic field, which produces enough effects by heating the tissue in which MNPs accumulate. When a tumor is subjected to high temperatures of heat > 46°C, it will cause cells to undergo direct tissue necrosis. From what has been mentioned above, the answer to the problem if magnetic hyperthermia can be applied to cancer therapy depends on the sufficient concentrations and the high enough frequency and power.⁴³ Compared with hyperthermia treatment, the LFAMF used in our new tumor therapy has a very low frequency and power, which makes the temperature change in a very small range.⁴⁴ In addition, the concentrations of MNPs used in the experiments were smaller than that in hyperthermia treatment, which also reduced the heat generated. The temperature in the plates was already measured during the experiments. We found it changed in less than 3°C. Based on the above reasons, the method to keep the temperature of the plate suspending tumor cells was not designed before, but it might be needed in future study.

It is natural to believe that we should not ignore the size and the property of the magnetic particle because of the efficiency of delivery and available magnetic force. Larger magnetic particles, such as micro beads, can be used to produce more force by an external field. But they require a different mechanism for delivery, such as an injection, which has an adverse effect on cells. On the other hand, smaller particles, such as paramagnetic nanoparticles, can be delivered relatively easily by endocytosis. However, the amount of force that can be exerted by an external field is very small. Based on this, the question

that what size of MNP-Fe₃O₄ could be our best choice becomes one of our important tasks, as well as how to achieve results more effectively. Much more research is needed.

5. Conclusion

It was demonstrated that tumor cells growth was modulated by the cooperation of internalized MNP-Fe₃O₄ and the external exposure of LFAMF. The following conclusions could be obtained:

- (1) LFAMF does not cause damage to cells, and MNP-Fe₃O₄ was proved to be safe in clinical medicine.
- (2) LFAMF can drive the MNP-Fe₃O₄ to damage tumor cells significantly by destroying the integrity of cell membrane, and the effect is in connection with the time and power.

In short, it can be said that we find an unconventional approach for cancer treatment using the physical therapy. By further improvement, it is expected that a new cancer treatment instrument will be developed by combining the magnetic field control technology with magnetic targeting. One of its most promising advantages is that it may significantly diminish the problems associated with chemical toxicity and harmful radiation. This approach could greatly facilitate future biomedical applications of nanoparticles.

Acknowledgments

We acknowledge the support by funding of Jiangsu Innovation Program for Graduate Education (KYLX_0247) and the support of the Fundamental Research Funds for the Central Universities.

References

1. S. Laurent, D. Forge, M. Port, A. Roch, A. Robic, L. V. Elst, R. N. Muller, "Magnetic iron oxide nanoparticles: Synthesis, stabilization, vectorization, physicochemical characterizations and biological applications," *Chem. Rev.* **108**, 2064–2110 (2008).
2. S. Mornet, S. Vasseur, F. Grasset, E. Duguet, "Magnetic nanoparticle design for medical diagnosis and therapy," *J. Mater. Chem.* **14**, 2161–2175 (2004).
3. E. Katz, I. Willner, "Integrated nanoparticle-biomolecule hybrid systems: Synthesis, properties, and applications," *Angew Chem.* **43**, 6042–6108 (2004).
4. T. Matsunaga, Y. Okamura, T. Tanaka, "Biotechnological application of nano-scale engineered bacterial magnetic particles," *J. Mater. Chem.* **14**, 2099–2105 (2004).
5. H. Oliveira, E. Pérez-Andrés, J. Thevenot, O. Sandre, E. Berra, S. Lecommandoux, "Magnetic field triggered drug release from polymersomes for cancer therapeutics," *J. Controlled Release* **169**, 165–170 (2013).
6. M. Mahmoudi, A. Simchi, M. Imani, P. Stroeve, A. Sohrabi, "Templated growth of superparamagnetic iron oxide nanoparticles by temperature programming in the presence of poly (vinyl alcohol)," *Thin Solid Films* **518**, 4281–4289 (2010).
7. M. Mahmoudi, S. Sant, B. Wang, S. Laurent, T. Sen, "Superparamagnetic iron oxide nanoparticles (SPIONs): Development, surface modification and applications in chemotherapy," *Adv. Drug. Deliv. Rev.* **63**, 24–46 (2011).
8. A. K. Gupta, R. R. Naregalkar, V. D. Vaidya, M. Gupta, "Recent advances on surface engineering of magnetic iron oxide nanoparticles and their biomedical applications," *Nanomedicine* **2**, 23–39 (2007).
9. S. Lee, M. T. Harris, "Surface modification of magnetic nanoparticles capped by oleic acids: Characterization and colloidal stability in polar solvents," *J. Colloid Interface Sci.* **293**, 401–408 (2006).
10. M. Arrueboa, R. Fernández-Pacheco, M. R. Ibarra, J. Santamaria, "Magnetic nanoparticles for drug delivery," *Nano Today* **2**, 22–32 (2007).
11. M. Johannsen, U. Gneveckow, L. Eckelt, A. Feussner, N. Waldöfner, R. Scholz, S. Deger, P. Wust, S. A. Loening, A. Jordan, "Clinical hyperthermia of prostate cancer using magnetic nanoparticles: Presentation of a new interstitial technique," *Int. J. Hyperthermia* **21**, 637–647 (2005).
12. M. M. Yallapu, S. F. Othman, E. T. Curtis, B. K. Gupta, M. Jaggi, S. C. Chauhan, "Multi-functional magnetic nanoparticles for magnetic resonance imaging and cancer therapy," *Biomaterials* **32**, 1890–1905 (2011).
13. R. Frade, S. Simeonov, A. Rosatella, F. Siopa, C. Afonso, "Toxicological evaluation of magnetic ionic liquids in human cell lines," *Chemosphere* **92**, 100–105 (2013).
14. K. Müller *et al.*, "Effect of ultrasmall superparamagnetic iron oxide nanoparticles (ferumoxtran-10) on human monocyte-macrophages in vitro," *Biomaterials* **28**, 1629–1642 (2007).
15. H. Hejase, S. S. Hayek, S. Qadri, Y. Haik, "MnZnFe nanoparticles for self-controlled magnetic hyperthermia," *J. Magn. Magn. Mater.* **324**, 3620–3628 (2010).

16. S. Laurent, S. Dutz, U. O. Häfeli, M. Mahmoudi, "Magnetic fluid hyperthermia: Focus on superparamagnetic iron oxide nanoparticles," *Adv. Colloid Interface Sci.* **166**, 8–23 (2011).
17. C. S. S. R. Kumar, F. Mohammad, "Magnetic nanomaterials for hyperthermia-based therapy and controlled drug delivery," *Adv. Drug. Deliv. Rev.* **63**, 789–808 (2011).
18. A. K. Gupta, M. Gupta, "Synthesis and surface engineering of iron oxide nanoparticles for biomedical applications," *Biomaterials* **26**, 3995–4021 (2005).
19. D. Chan, D. Kirpotin, P. A. Bunn, "Synthesis and evaluation of colloidal magnetic iron-oxides for the site-specific radiofrequency-induced hyperthermia of cancer," *J. Magn. Magn. Mater.* **122**, 374–378 (1993).
20. A. Jordan, P. Wust, H. Fähling, W. John, A. Hinz, R. Felix, "Inductive heating of ferromagnetic particles and magnetic fluids: Physical evaluation of their potential for hyperthermia," *Int. J. Hyperthermia* **9**, 51–68 (1993).
21. E. Neumann, M. Schaefer-Ridder, Y. Wang, P. H. Hofschneider, "Gene transfer into mouse lymphoma cells by electroporation in high electric fields," *EMBO J.* **1**, 841–845 (1982).
22. P. Kocbek, S. Kralj, M. E. Kreft, J. Kristl, "Targeting intracellular compartments by magnetic polymeric nanoparticles," *European Journal of Pharmaceutical Sciences* **50**, 130–138 (2013).
23. E. Jang, J. Shin, G. Ren, M. Park, K. Cheng, X. Chen, J. C. Wu, J. B. Sunwoo, Z. Cheng, "The manipulation of natural killer cells to target tumor sites using magnetic nanoparticles," *Biomaterials* **33**, 5584–5592 (2013).
24. D. Baba, Y. Seiko, T. Nakanishi, H. Zhang, A. Arakaki, T. Matsunaga, T. Osaka, "Effect of magnetite nanoparticles on living rate of MCF-7 human breast cancer cells," *Colloids Surf B: Biointerfaces* **95**, 254–257 (2012).
25. R. E. Rosensweig "Heating magnetic fluid with alternating magnetic field," *J. Magn. Magn. Mater.* **252**, 370–374 (2002).
26. R. W. Rand, H. D. Snow, D. G. Elliott, G. M. Haskins, "Induction heating method for use in causing necrosis of neoplasm," Patent US4545368 (1985).
27. M. Faraji, Y. Yamini, M. Rezaee, "Magnetic nanoparticles: Synthesis, stabilization, functionalization, characterization, and applications," *J. Iran. Chem. Soc.* **7**, 1–37 (2010).
28. I. Brigger, C. Dubernet, P. Couvreur, "Nanoparticles in cancer therapy and diagnosis," *Adv. Drug. Deliv. Rev.* **54**, 631–651 (2002).
29. A. Marcu, S. Pop, F. Dumitrache, M. Mocanu, C. M. Niculite, M. Gherghiceanu, C. P. Lungu, C. Fleaca, R. Ianchis, A. Barbut, C. Grigoriu, I. Morjan, "Magnetic iron oxide nanoparticles as drug delivery system in breast cancer," *Applied Surface Science* **281**, 60–65 (2013).
30. J. Xu, K. Mahajanm, W. Xue, J. O. Winter, M. Zborowski, J. J. Chalmers, "Simultaneous, single particle, magnetization and size measurements of micron sized, magnetic particles," *J. Magn. Magn. Mater.* **324**, 4189–4199 (2012).
31. J. Bae, M. Huh, B. Ryu, J. Do, S. Jin, M. Moon, J. Jung, Y. Chang, E. Kim, S. Chi, G. Lee, K. Chae, "The effect of static magnetic fields on the aggregation and cytotoxicity of magnetic nanoparticles," *Biomaterials* **32**, 9401–9414 (2011).
32. Y. Wei, B. Han, X. Hu, Y. Lin, X. Wang, X. Deng, "Synthesis of Fe₃O₄ nanoparticles and their magnetic properties," *Procedia Engineering* **27**, 632–637 (2012).
33. J. K. Hsiao, H. H. Chu, Y. H. Wang, C. W. Lai, P. T. Chou, S. T. Hsieh, J. L. Wang, H. M. Liu, "Macrophage physiology function after superparamagnetic iron oxide labeling," *NMR Biomed* **21**, 820–829 (2008).
34. T. Mosmann, "Rapid colorimetric assay for cellular growth and survival: Application to proliferation and cytotoxicity assays," *J. Immunol. Methods* **65**, 55–63 (1983).
35. M. S. Cartiera, K. M. Johnson, V. Rajendran, M. J. Caplan, W. M. Saltzman, "The uptake and intracellular fate of PLGA nanoparticles in epithelial cells," *Biomaterials* **30**, 2790–2798 (2009).
36. G. Li, D. Li, L. Zhang, J. Zhang, E. Wang, "One-step synthesis of folic acid protected gold nanoparticles and their receptor-mediated intracellular uptake," *Chemistry* **15**, 9868–9873 (2009).
37. C. Fanelli, S. Coppola, R. Barone, C. Colussi, G. Gualandi, P. Volpe L. Ghibelli, "Magnetic fields increase cell survival by inhibiting apoptosis via modulation of Ca²⁺ influx," *FASEB J.* **13**, 95–102 (1999).
38. J. Shin, C. Yoo, J. Lee, M. Cha, "Cell response induced by internalized bacterial magnetic nanoparticles under an external static magnetic field," *Biomaterials* **33**, 5650–5657 (2012).
39. M. Simko, M. O. Mattsson, "Extremely low frequency electromagnetic fields as effectors of cellular responses in vitro: Possible immune cell activation," *J. Cell Biochem* **93**, 83–92 (2004).
40. D. Stratton, S. Lange, J. M. Inal, "Pulsed extremely low-frequency magnetic fields stimulate microvesicle release from human monocyticleukaemia cells," *Biochem. Biophys. Res. Commun.* **430**, 470–475 (2013).
41. J. Zhao, M. Deng, J. Zeng, Z. Huang, G. Yin, X. Liao, J. Gu, J. Huang, "Preparation of Fe₃O₄

- and CoFe_2O_4 nanoparticles with cellular compatibility via the histidine assistance,” *Colloids Surf. A: Physicochem. Eng. Asp.* **401**, 54–60 (2012).
42. N. V. Jadhav, A. I. Prasad, A. Kumar, R. Mishra, S. Dhara, K. R. Babu, C. L. Prajapat, N. L. Misra, R. S. Ningthoujam, B. N. Pandey, R. K. Vatsa, “Synthesis of oleic acid functionalized Fe_3O_4 magnetic nanoparticles and studying their interaction with tumor cells for potential hyperthermia applications,” *Colloids Surf. B Biointerfaces* **108**, 158–168 (2013).
 43. S. Kossatz, R. Ludwig H. Dahring, V. Ettelt, G. Rinkus, M. Marciello, G. Salas, V. Patel, F. J. Teran, I. Hilger “High therapeutic efficiency of magnetic hyperthermia in xenograft models achieved with moderate temperature dosages in the tumor area,” available at <http://link.springer.com> (2014).
 44. K. Murase, H. Takata, Y. Takeuchi, S. Saito, “Control of the temperature rise in magnetic hyperthermia with use of an external static magnetic field,” *Phys. Med.* **29**, 624–630 (2013).